Revealing governing mechanisms in hydraulic stimulation of geothermal reservoirs by mathematical and numerical modelling

Inga Berre

UNIVERSITY OF BERGEN

University of Bergen Porous media group research activities – an illustration of the energy transition in geosciences

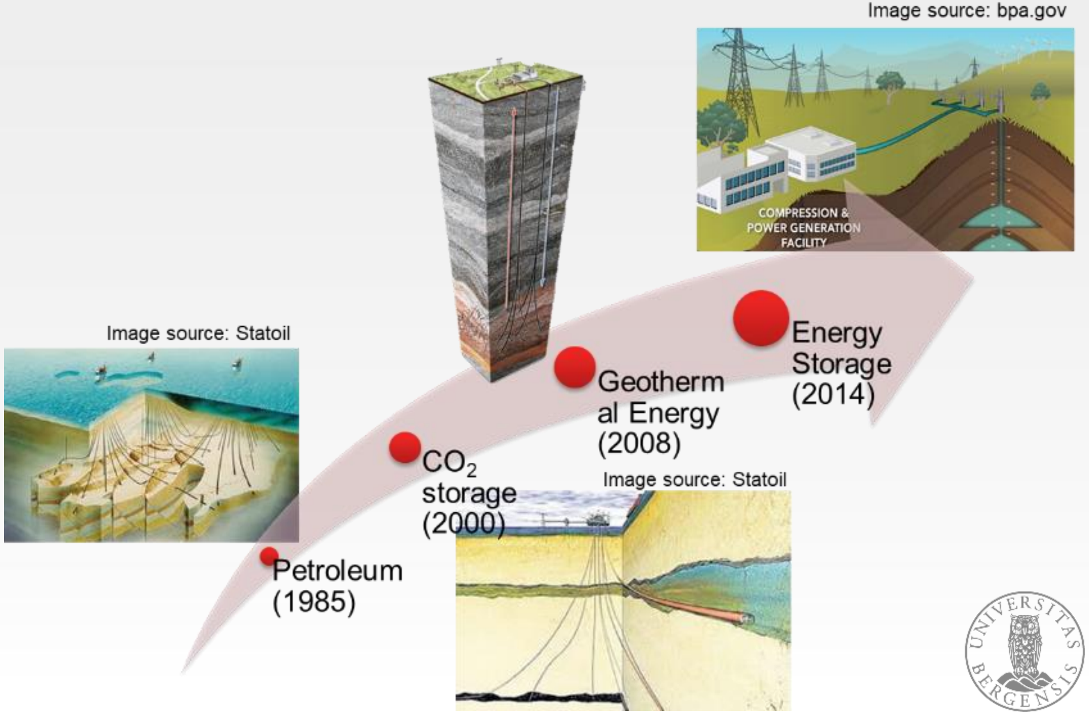

Computational geoscience

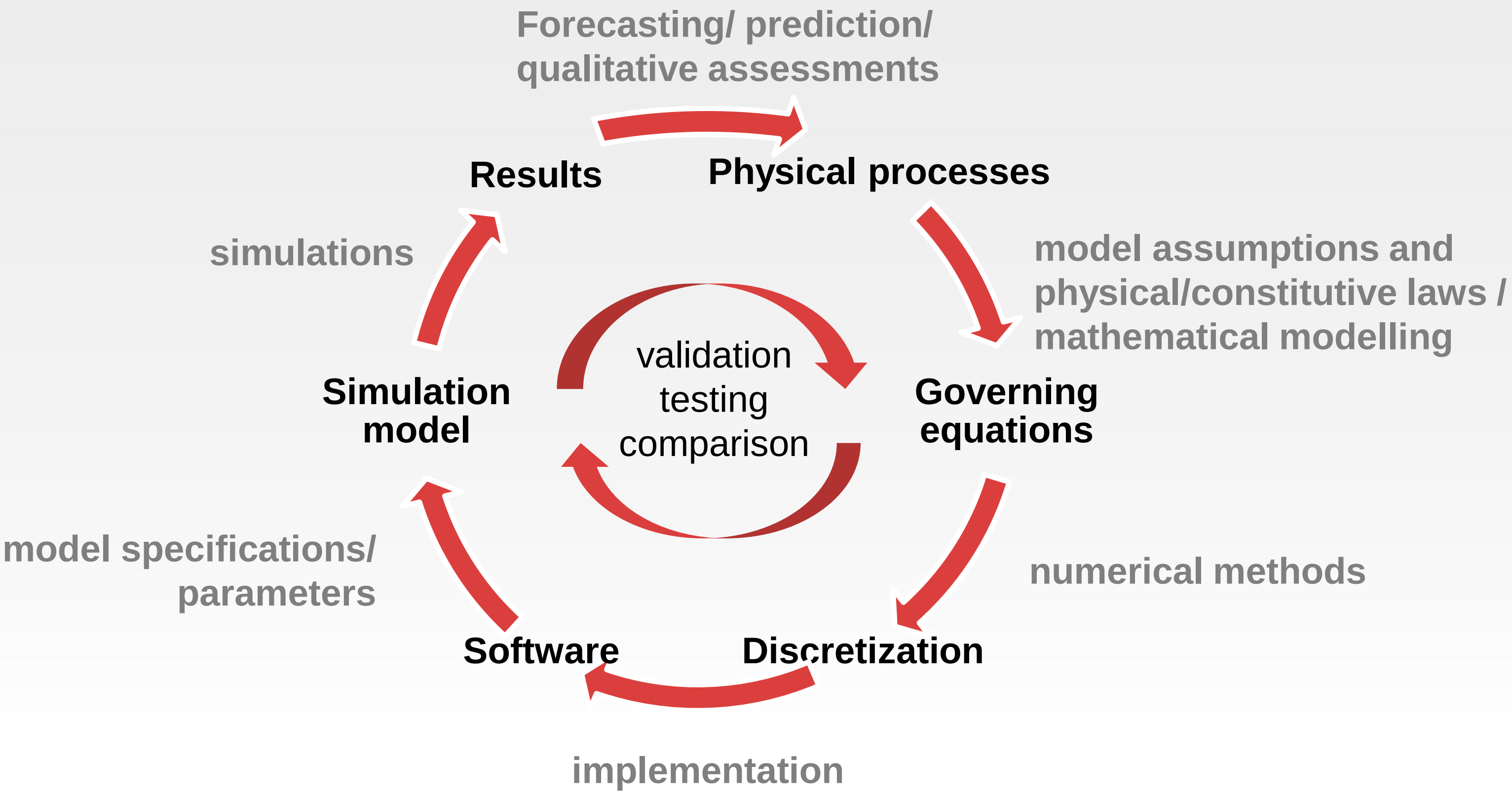

Geothermal systems

Utilization of deep geothermal sources requires sufficient

- heat
- fluid
- permeability

Resource types

- conventional hydrothermal
- **enhanced geothermal systems**
- superheated / supercritical

Enhanced geothermal systems
- Hydraulic stimulation by shear dilation

- Natural fractures already exist
- Large difference between maximum and minimum horizontal stress
- Prior stable situation due to friction between fracture surfaces
- Injection of fluid at elevated pressures results in slip and dilation

Inject water

Decrease frictional resistance

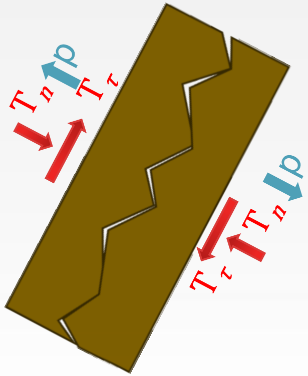

The relative displacement of the fracture's surfaces with slip results in dilation of the fracture

Hydraulic stimulation measurements in lab and field

Lab-measurements of fracture permeability under shear and normal load

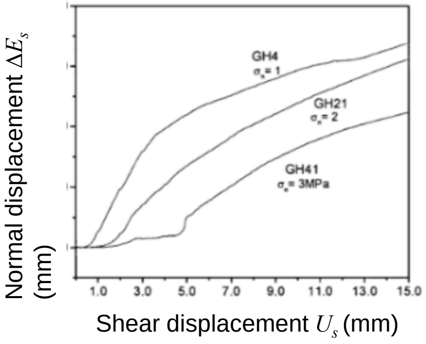

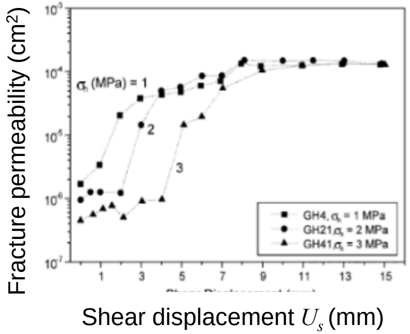

Lee and Cho, *Rock Mech Rock Engng*, 2002

Measurement of fault slip and permeability enhancement induced by fluid injection into a natural fault

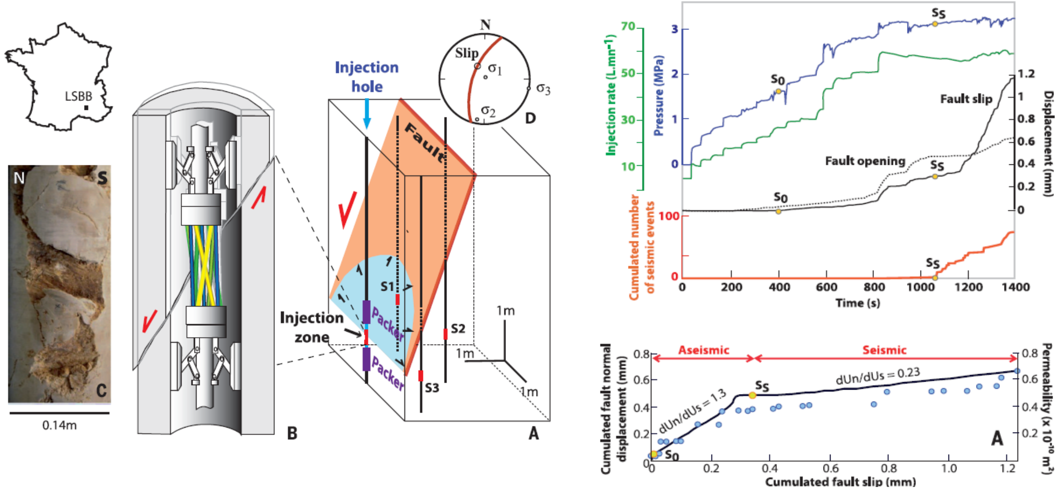

Guglielmi, Cappa, Avouac, Henry, Elsworth, *Science*, 2015

Induced Seismicity

- In hydraulic stimulation, seismicity is deliberately induced
- Generally M_L< 3.0 (micro earthquake)
- Larger earthquakes must be avoided

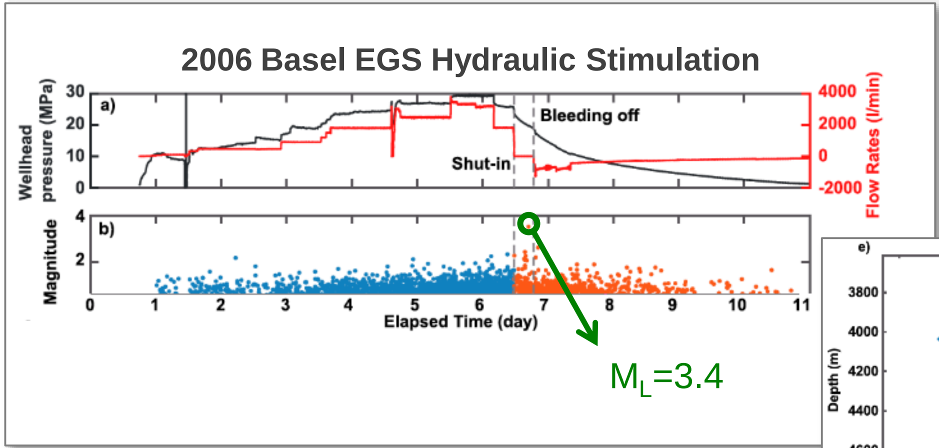

Figure source: Mukuhira et al., *J. Geophys Res Solid Earth*, 2017

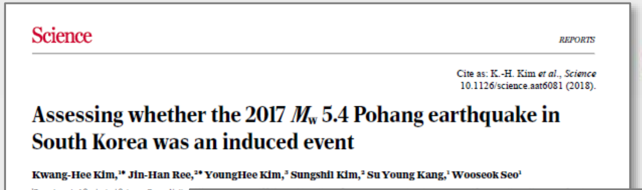
Science REPORTS

Cite as: K.-H. Kim *et al.*, *Science* 10.1126/science.aat6081 (2018).

Assessing whether the 2017 M_w 5.4 Pohang earthquake in South Korea was an induced event

Kwang-Hee Kim,[1]* Jin-Han Ree,[2]* YoungHee Kim,[3] Sungshil Kim,[3] Su Young Kang,[1] Wooseok Seo[1]

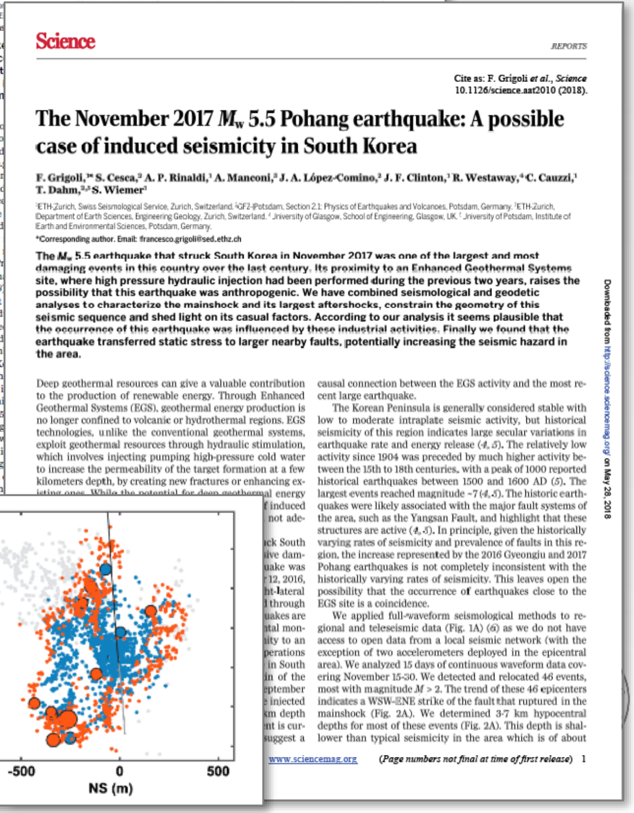
Science REPORTS

Cite as: F. Grigoli *et al.*, *Science* 10.1126/science.aat2010 (2018).

The November 2017 M_w 5.5 Pohang earthquake: A possible case of induced seismicity in South Korea

F. Grigoli,[1]* S. Cesca,[2] A. P. Rinaldi,[1] A. Manconi,[3] J. A. López-Comino,[2] J. F. Clinton,[1] R. Westaway,[4] C. Cauzzi,[1] T. Dahm,[2,5] S. Wiemer[1]

The M_w 5.5 earthquake that struck South Korea in November 2017 was one of the largest and most damaging events in this country over the last century. Its proximity to an Enhanced Geothermal Systems site, where high pressure hydraulic injection had been performed during the previous two years, raises the possibility that this earthquake was anthropogenic. We have combined seismological and geodetic analyses to characterize the mainshock and its largest aftershocks, constrain the geometry of this seismic sequence and shed light on its casual factors. According to our analysis it seems plausible that the occurrence of this earthquake was influenced by these industrial activities. Finally we found that the earthquake transferred static stress to larger nearby faults, potentially increasing the seismic hazard in the area.

Deep geothermal resources can give a valuable contribution to the production of renewable energy. Through Enhanced Geothermal Systems (EGS), geothermal energy production is no longer confined to volcanic or hydrothermal regions. EGS technologies, unlike the conventional geothermal systems, exploit geothermal resources through hydraulic stimulation, which involves injecting pumping high-pressure cold water to increase the permeability of the target formation at a few kilometers depth, by creating new fractures or enhancing ex-

causal connection between the EGS activity and the most recent large earthquake.

The Korean Peninsula is generally considered stable with low to moderate intraplate seismic activity, but historical seismicity of this region indicates large secular variations in earthquake rate and energy release (4, 5). The relatively low activity since 1904 was preceded by much higher activity between the 15th to 18th centuries, with a peak of 1000 reported historical earthquakes between 1500 and 1600 AD (5). The largest events reached magnitude ~7 (4, 5). The historic earthquakes were likely associated with the major fault systems of the area, such as the Yangsan Fault, and highlight that these structures are active (4, 5). In principle, given the historically varying rates of seismicity and prevalence of faults in this region, the increase represented by the 2016 Gyeongju and 2017 Pohang earthquakes is not completely inconsistent with the historically varying rates of seismicity. This leaves open the possibility that the occurrence of earthquakes close to the EGS site is a coincidence.

We applied full-waveform seismological methods to regional and teleseismic data (Fig. 1A) (6) as we do not have access to open data from a local seismic network (with the exception of two accelerometers deployed in the epicentral area). We analyzed 15 days of continuous waveform data covering November 15-30. We detected and relocated 46 events, most with magnitude M > 2. The trend of these 46 epicenters indicates a WSW-ENE strike of the fault that ruptured in the mainshock (Fig. 2A). We determined 3-7 km hypocentral depths for most of these events (Fig. 2A). This depth is shallower than typical seismicity in the area which is of about

www.sciencemag.org (Page numbers not final at time of first release) 1

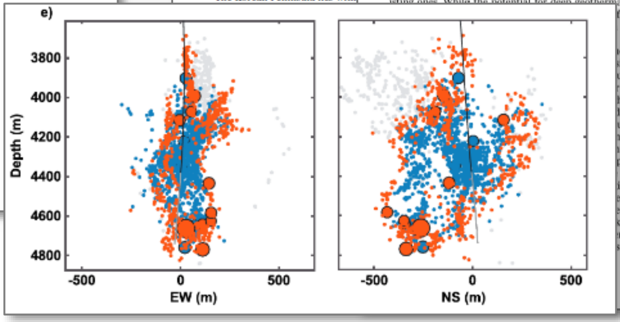

Mathematical modeling
– coupled processes

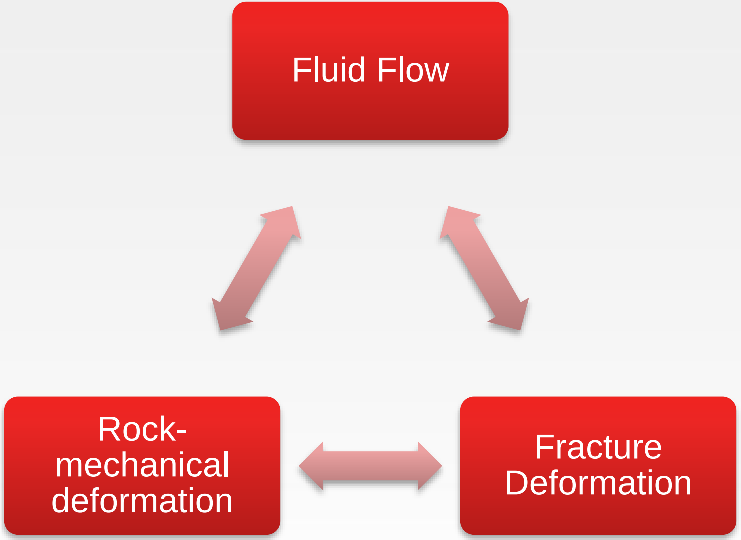

Ucar, Berre, Keilegavlen (*Geophys Res Lett*, 2017)

Structure

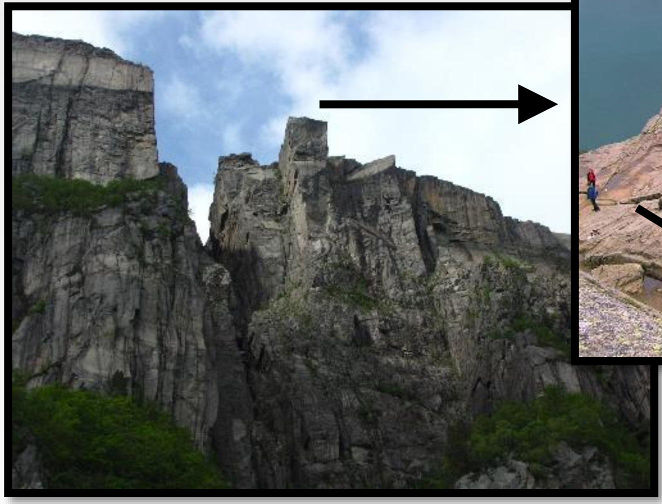

Credits: A. Gohr

Credits: Stavanger Aftenblad

different scales – complex structure

Mathematical modeling
- representation of fractures

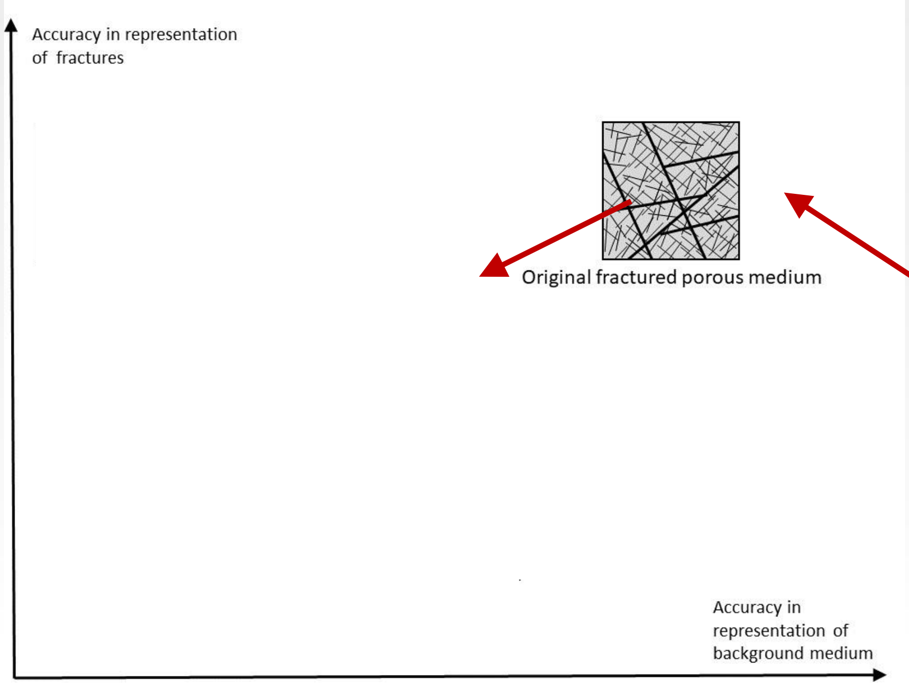

B, Keilegavlen & Doster, *Transport in Porous Media*, 2018

Modeling - Flow

Assumptions: single-phase, weakly compressible fluid

Conservation of Mass

$$\phi c \frac{\partial p}{\partial t} + \nabla \cdot \mathbf{w} = q, \qquad \mathbf{x} \in \Omega_\mathrm{m} \in R^3$$

$$\phi_f c \frac{\partial p}{\partial t} + \nabla^{\parallel} \cdot \mathbf{w}_\mathrm{f}^{\parallel} = q_f + \frac{1}{d_\mathrm{n}}\left(w_{\Gamma^+}^{\perp} + w_{\Gamma^-}^{\perp}\right), \qquad \mathbf{x} \in \Omega_\mathrm{f} \in R^2$$

Darcy velocity

$$\mathbf{w} = -\frac{\mathbf{K}}{\mu}\nabla p, \qquad \mathbf{x} \in \Omega_\mathrm{m} \in R^3$$

$$\mathbf{w}_\mathrm{f}^{\parallel} = -\frac{\mathbf{K}_\mathrm{f}^{\parallel}}{\mu}\nabla^{\parallel}\mathrm{p}, \qquad \mathbf{x} \in \Omega_\mathrm{f} \in R^2$$

Cubic law

$$K_f = \frac{e^2}{12}.$$

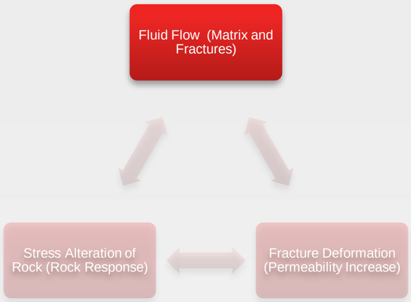

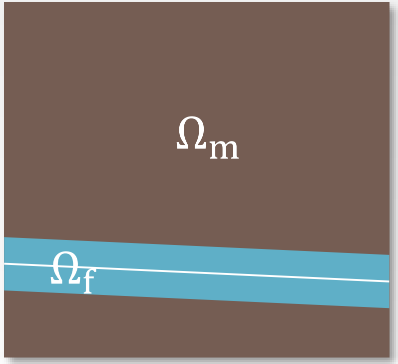

Numerical approach

- Fractures are treated as co-dimension one
- Cell-centered finite-volume method (two-point flux approximation).

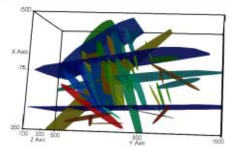

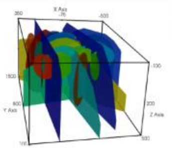

Flemisch, B, Boon, Fumagalli, Schwenck, Scotti, Stefansson & Tatomir. *Adv Water Res*, 2018
Stefansson, B and Keilegavlen. *Transport in Porous Media*, 2018

Fracture deformation

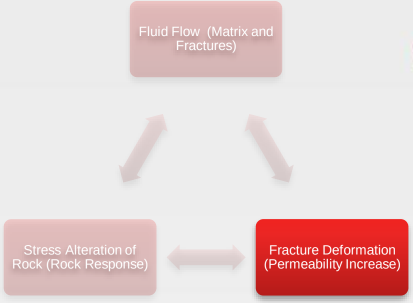

Static/dynamic friction model
Mohr–Coloumb criterion

$$|\boldsymbol{\tau}| < \mu_s(\sigma_\mathrm{n} - p) \rightarrow [d_s] = 0$$
$$x \in \Gamma_f \backslash \Gamma_s$$

$$|\boldsymbol{\tau}| = \mu_d(\sigma_\mathrm{n} - p) \rightarrow [d_s] = \alpha\boldsymbol{\tau},\ \alpha > 0$$
$$x \in \Gamma_s$$

$$\mu_d < \mu_s$$

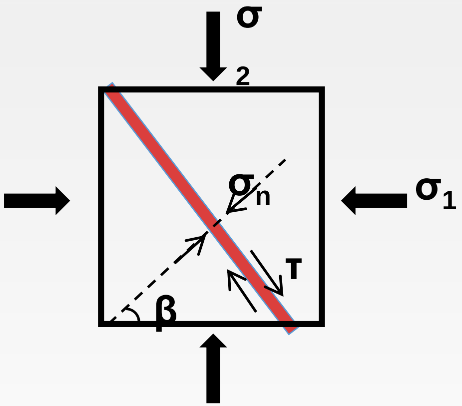

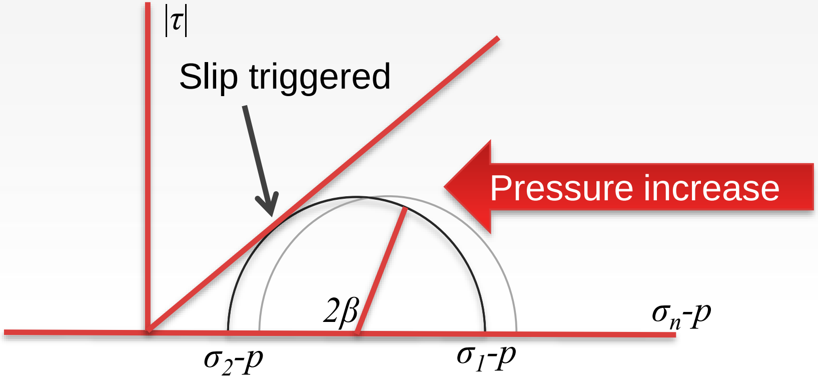

Fracture deformation

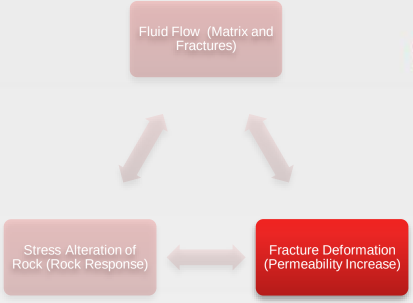

Dilation:

$$d_{\mathrm{n}} = E_0 - E_{\mathrm{e}} + E_{\mathrm{s}}$$

$$E_{\mathrm{s}} = d_s \tan \varphi_{\mathrm{dil}},$$

Hydraulic aperture

$$e = \frac{{d_{\mathrm{n}}}^2}{JRC^{2.5}}$$

Fracture displacement:

$$\mathbf{u}_- - \mathbf{u}_+ = d_{\mathrm{n}} \mathbf{n}_+ + d_{\mathrm{s}} \boldsymbol{\zeta}_+$$

Approximated shear displacement (excess shear stress approximation):

$$[d_s] = \frac{|\boldsymbol{\tau}| - \mu_d(\sigma_{\mathrm{n}} - p)}{K_s}$$

Reversible normal deformation (Barton-Bandis):

$$E_e = \frac{-(\sigma_n - p)}{K_n + \dfrac{\sigma_n - p}{E_{\max}}}$$

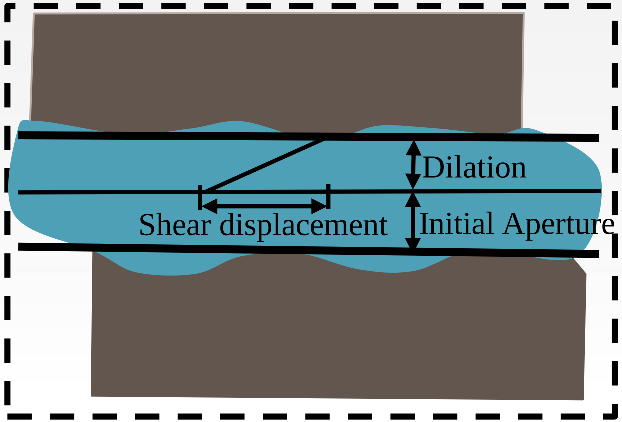

Stress response of matrix due to fracture deformation

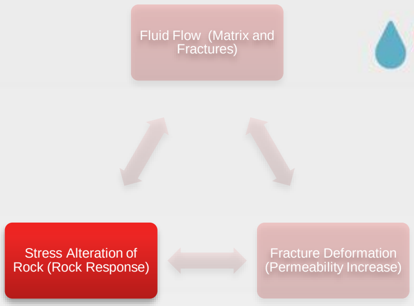

Assumptions: quasi-static problem, isotropic medium

Conservation of Momentum:

$$\nabla \cdot \boldsymbol{\sigma} = \mathbf{0},$$

Hooke's law

$$\boldsymbol{\sigma} = 2G\boldsymbol{\varepsilon} + \lambda \operatorname{tr}(\boldsymbol{\varepsilon})\mathbf{I},$$

$$\boldsymbol{\varepsilon} = \frac{\left(\nabla\mathbf{u} + (\nabla\mathbf{u}^T)\right)}{2},$$

Fracture deformations as conditions on internal boundaries

Numerical Approach

Cell-centered finite-volume method (MPSA) for fractured media

Ucar, Keilegavlen, B, Nordbotten, *Comput Geosci*, 2018

Hydro-mechanical coupling

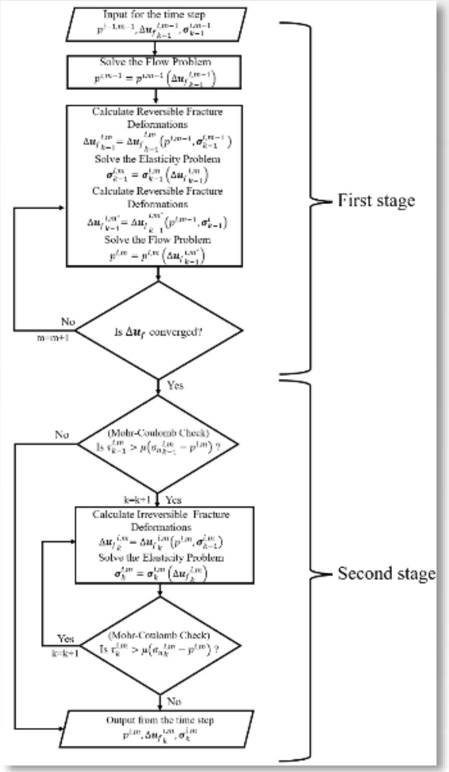

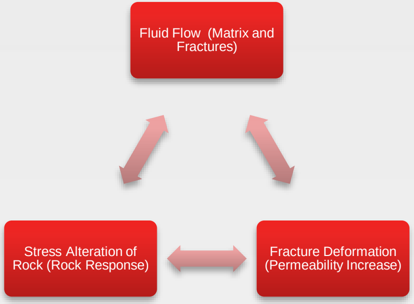

First stage: balance between fluid flow, reversible fracture deformation, stress response of the matrix

Second stage: capturing of the irreversible fracture deformation and stress response of the matrix

Ucar, B, Keilegavlen, *J Geophys Res Solid Earth*, 2018

Hydraulic stimulation results

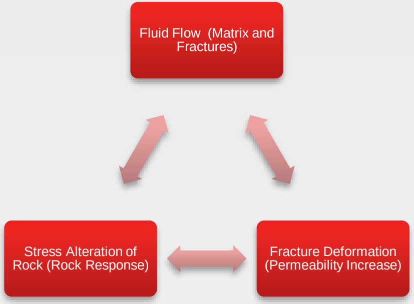

Fracture network with 20 fractures
in a porous medium domain.

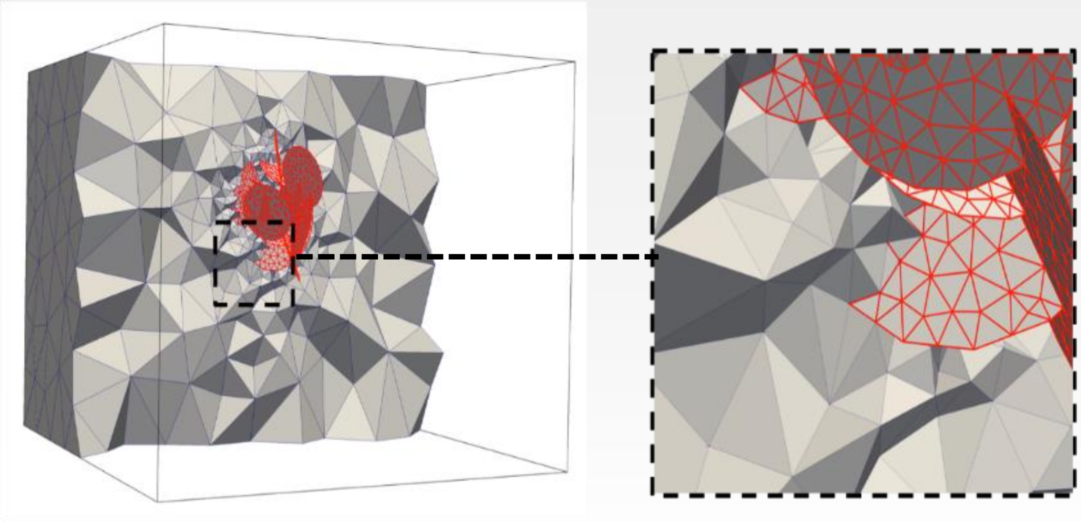

Ucar, B, Keilegavlen, *J Geophys Res Solid Earth*, 2018

Results: effect of background permeability

Permeability change and induced seismicity after 1 day of stimulation.

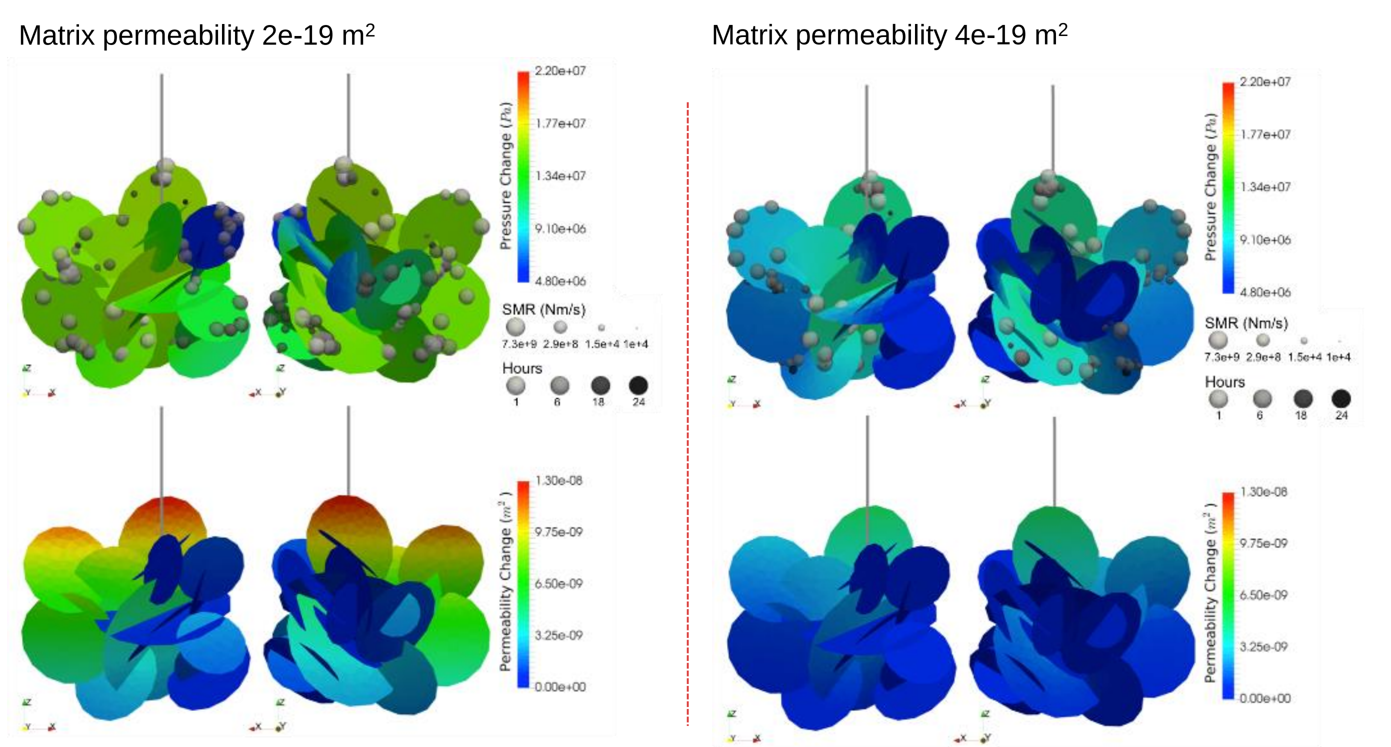

Ucar, B, and Keilegavlen, *J Geophys Res Solid Earth*, 2018

Postinjection seismicity due to reversible normal deformation of fractures

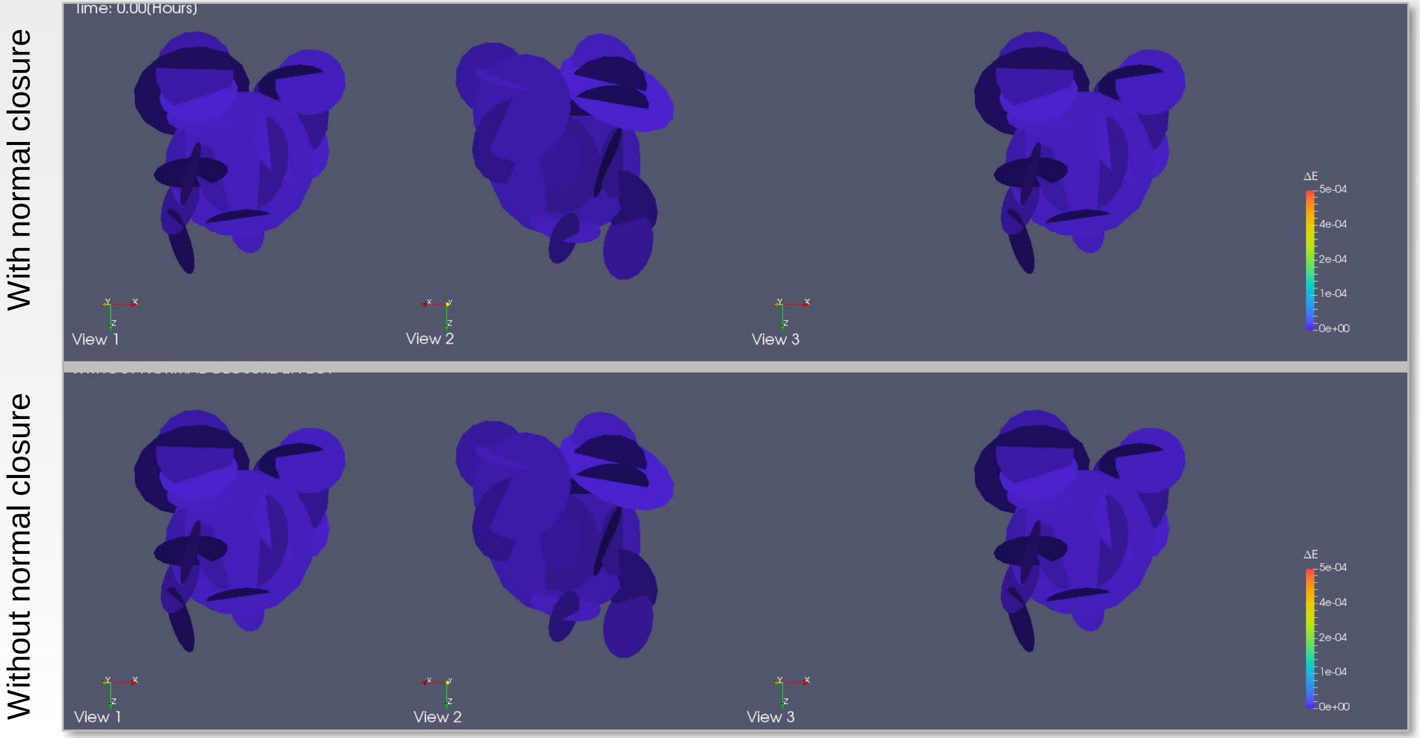

Ucar, B, Keilegavlen, *Geophys Res Lett*, 2017

Summary – modeling of hydraulic stimulation

- A numerical approach for simulation of shear stimulation of a complex fracture network in a 3d domain
  - DFM model; fluid flow in both fractures and matrix
- Factors that influence seismicity are studied
  - leakage into the rock matrix reduce seismicity
  - fracture closure is identified as a mechanism for postinjection seismicity

Main references

Ucar, B, Keilegavlen, *Geophys Res Lett*, 2017

Ucar, B, Keilegavlen, *J Geophys Res Solid Earth*, 2018

Recent improvements in modeling friction and contact mechanics

Shear test results

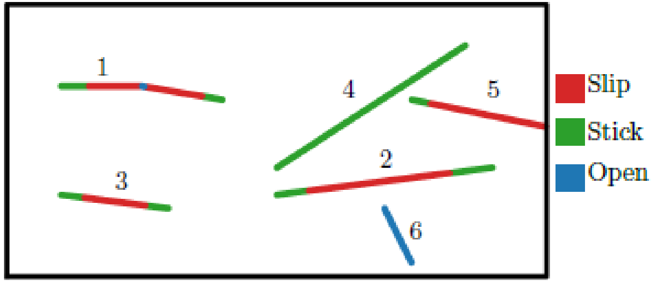

x-component of displacement

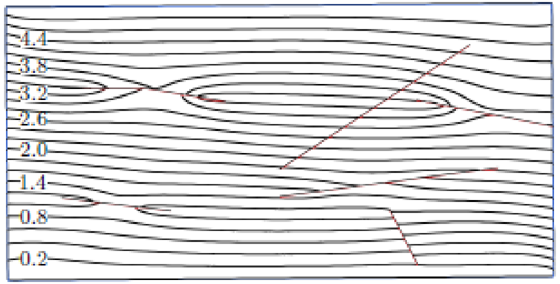

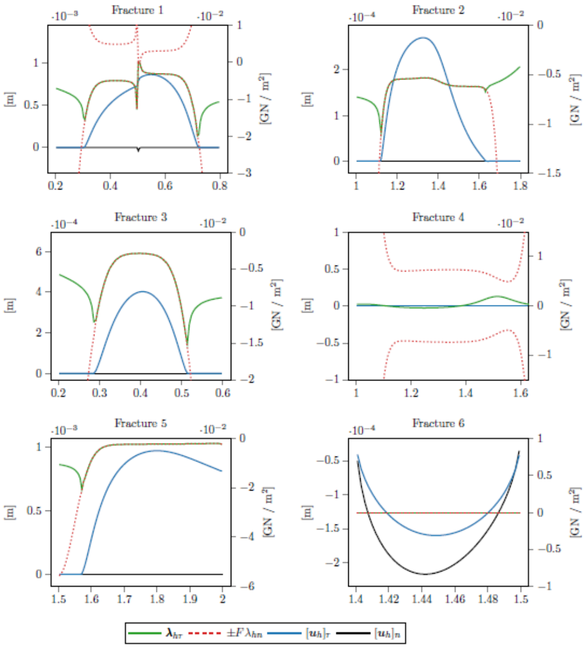

Berge, B., Keilegavlen, Nordbotten, Wohlmuth, arXiv:1904.11916 [math.NA], 2019

3D and poroelastic effects

3-D example

- bottom boundary: fixed,
- vertical boundaries: rolling,
- top boundary: Neumann load

Including fully coupled poroelasticity

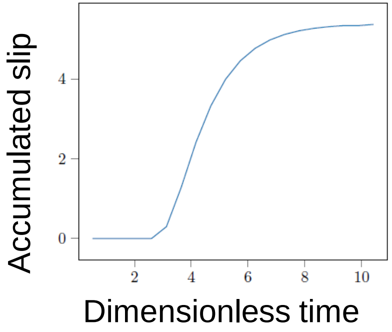

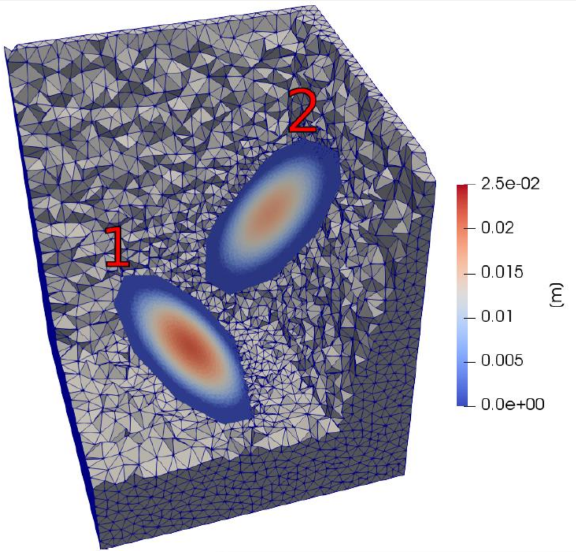

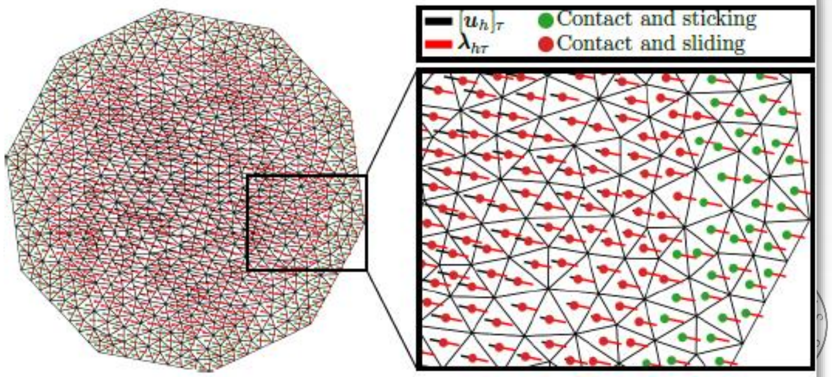

Berge, B., Keilegavlen, Nordbotten, Wohlmuth, arXiv:1904.11916 [math.NA], 2019

Ongoing work: mixed-mechanism stimulation

$$
\begin{cases}
\nabla \cdot \boldsymbol{\sigma} + \mathbf{b} = 0 & \text{in}\,\Omega \\
\boldsymbol{\sigma} = \mathbf{C} : \boldsymbol{\varepsilon} & \text{in}\,\Omega \\
\boldsymbol{\varepsilon} = \frac{1}{2}\left(\nabla \mathbf{u} + \nabla \mathbf{u}^{\mathrm{T}}\right) & \text{in}\,\Omega \\
\mathbf{u} = \bar{\mathbf{u}} & \text{on}\,\Gamma_{\mathbf{u}} \quad \text{Dirichlet BC} \\
\boldsymbol{\sigma} \cdot \mathbf{n} = \bar{\mathbf{t}} & \text{on}\,\Gamma_{\mathbf{t}} \quad \text{Neumann BC} \\
\mathbf{t} = 0 & \text{on}\,\Gamma_{c} \quad \text{Crack condition}
\end{cases}
$$

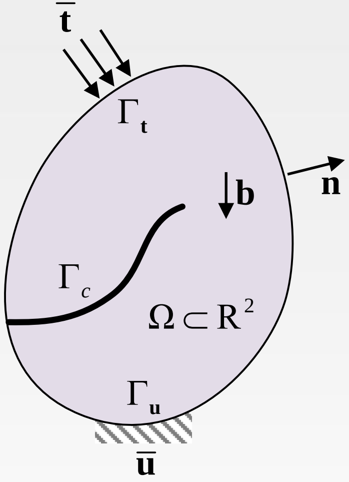

Crack tip: collapsed quarter point singular elements / Adaptive remeshing

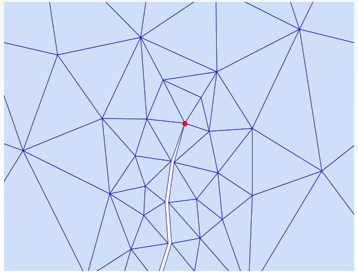

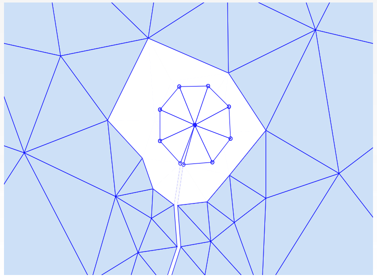

Quarter point elements around crack tip

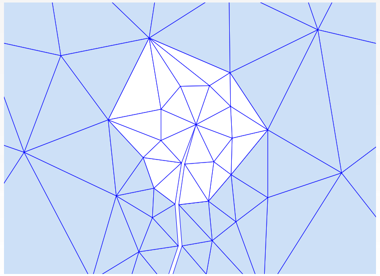

New mesh

Soghrati, Nagarajan. *Comput. Mech*, 2016

Wing-crack propagation results

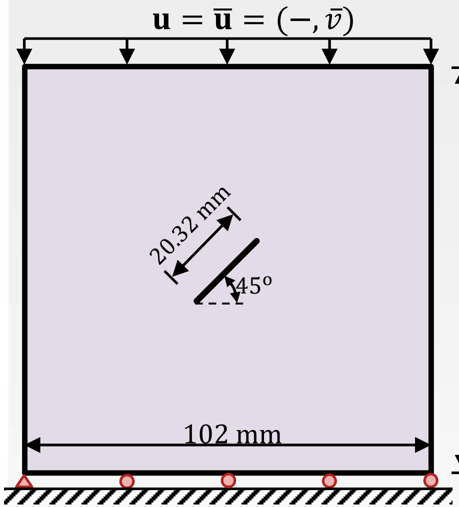

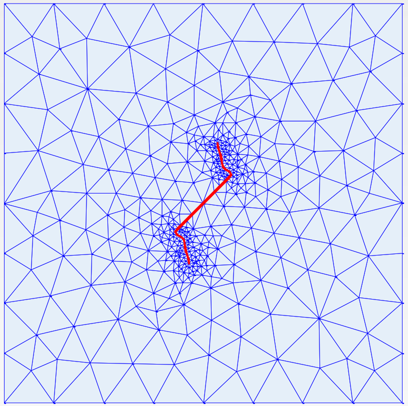

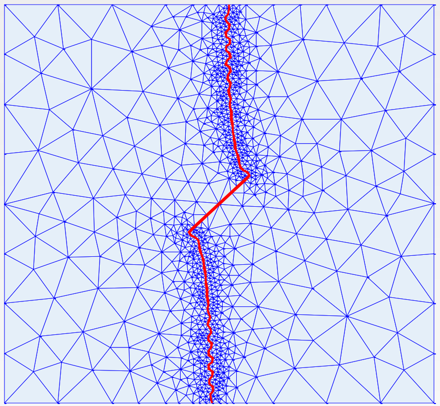

Hau, B and Keilegavlen, submitted European Geothermal Congress, 2019

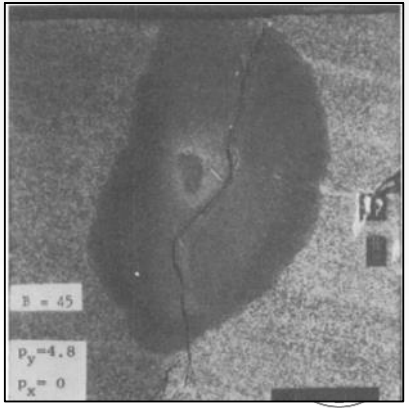

Ingraffea and Heuze, *Int. J. Numer. Anal. Methods Geomech.*,1980

Wing-crack propagation results

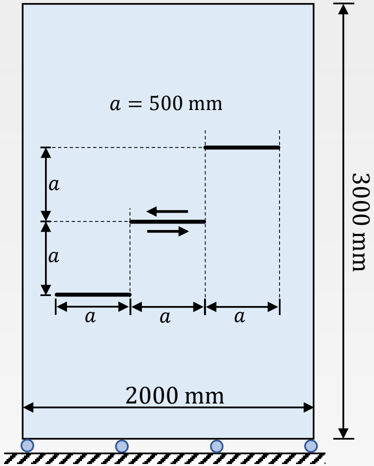

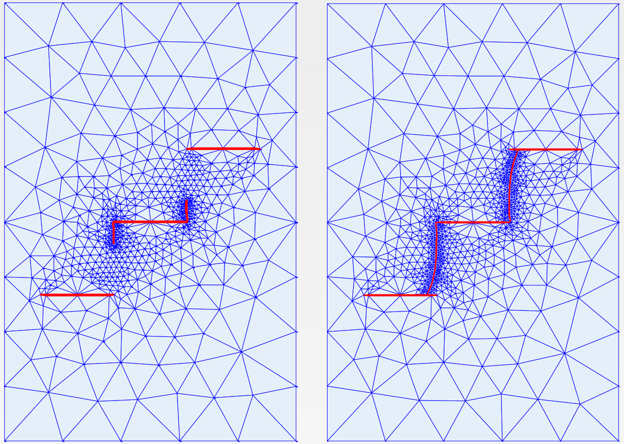

Hau, B and Keilegavlen, submitted European Geothermal Congress, 2019

What's next?

Further model and investigate effects of

- poroelasticity (Biot)

and then..

- thermoelasticity

Example

- Fractures induced by thermal shock (Fig.)

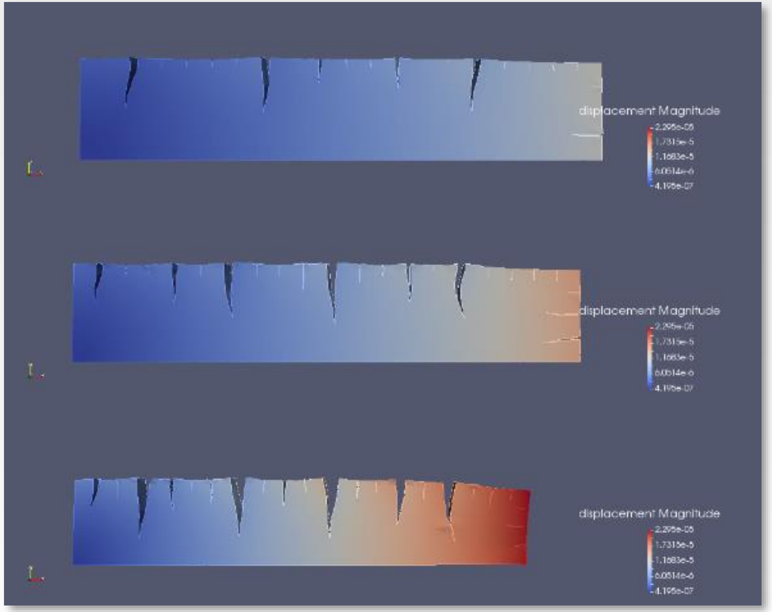

Stefansson, B, Keilegavlen, Paluszny. Unpublished, 2019

Acknowledgements

Runar Berge (UiB)
Eirik Keilegavlen (UiB)
Hau Trung Dang (UiB)
Michele Starnoni (UiB)
Ivar Stefansson (UiB)

Jan Nordbotten (UiB)
Alessio Fumagalli (UiB)
Michael Sargado (UiB)
Mats Brun (UiB)
Sæunn Halldorsdottir (ISOR/UiB)

Eren Ucar (UiB)
Florian Doster (Heriot-Watt)
Adriana Paluszny (Imperial College
Barbara Wohlmuth (Univ. Munich)
Volker Oye (NORSAR)
Bernd Flemisch (Univ. Stuttgart)

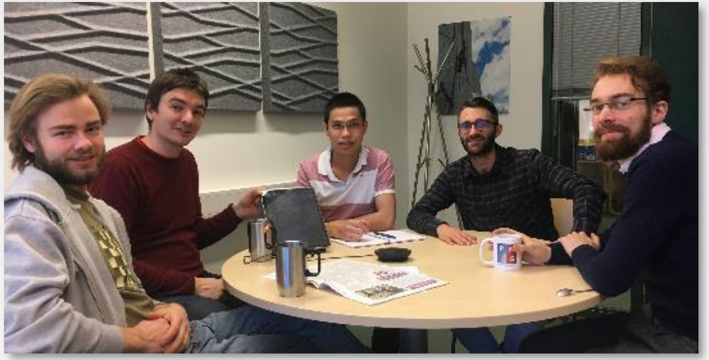

The Research Council of Norway

With funding from
The Research Council of Norway

equinor

GeoStim project, Research Council of Norway grant no. 228832
ERiS project, Research Council of Norway grant no. 267908

Open-source code: github.com/pmgbergen/porepy

Governing equations

Fracture criteria

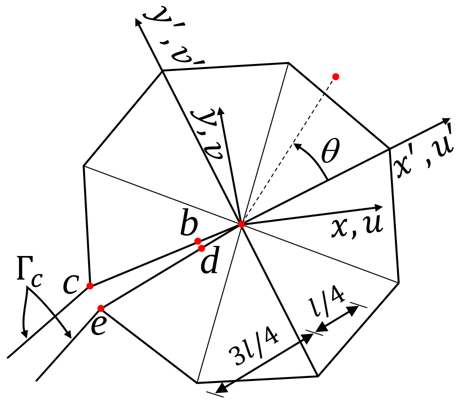

Collapsed quarter point singular elements - CQPE

1. **Maximum tangential stress: MTS**
2. Minimum strain energy density: MSE
3. Maximum potential energy release rate: ERR
4. Maximum dilatational strain energy density: T-cr
5. Maximum stress triaxiality: M-cr
6. Minimum distance from the crack tip to the core region boundary: R-cr
7. …

$$f\left(K_I, K_{II}, \theta\right) = 0 \quad \text{vs} \quad g\left(K_I, K_{II}, \theta\right) > 0$$

$$K_{eq}\left(\theta, K_I, K_{II}, l\right) \geq K_{IC}$$

K_I, K_{II} are the stress intensity factors

$$\begin{Bmatrix} K_I \\ K_{II} \end{Bmatrix} = \frac{E}{3(1+v)(1+k)} \sqrt{\frac{2\pi}{l}} \frac{1}{2} \begin{Bmatrix} 8(v_b' - v_d') - (v_c' - v_e') \\ 8(u_b' - u_d') - (u_c' - u_e') \end{Bmatrix}$$

S.S. Bhadauria, K.K. Pathak, M.S. Hora." Finite Element Modeling of Crack Initiation Angle Under Mixed Mode (I/II) Fracture ". Journal of Solid Mechanics Vol. 2, No. 3 (2010)

R. S. Barsoum, "On the use of isoparametric finite elements in linear fracture mechanics," Int. J. Numer. Methods Eng., 1976

R. D. Henshell and K. G. Shaw, "Crack tip finite elements are unnecessary," Int. J. Numer. Methods Eng., 1975

Discretization

Adaptive Remeshing

Laplacian smoothing

$$z^{*} = \frac{1}{n}\sum_{i=1}^{n} z_n$$

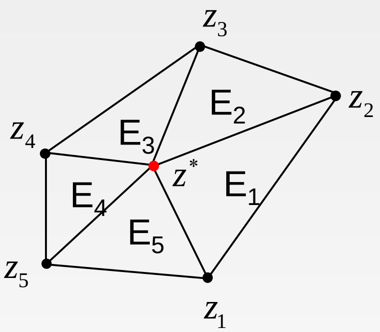

Refine vs Remesh processes

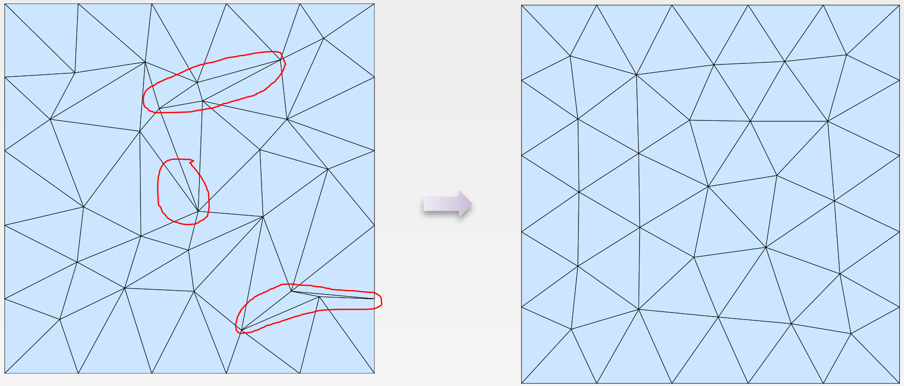

Process sequences of crack propagation simulation

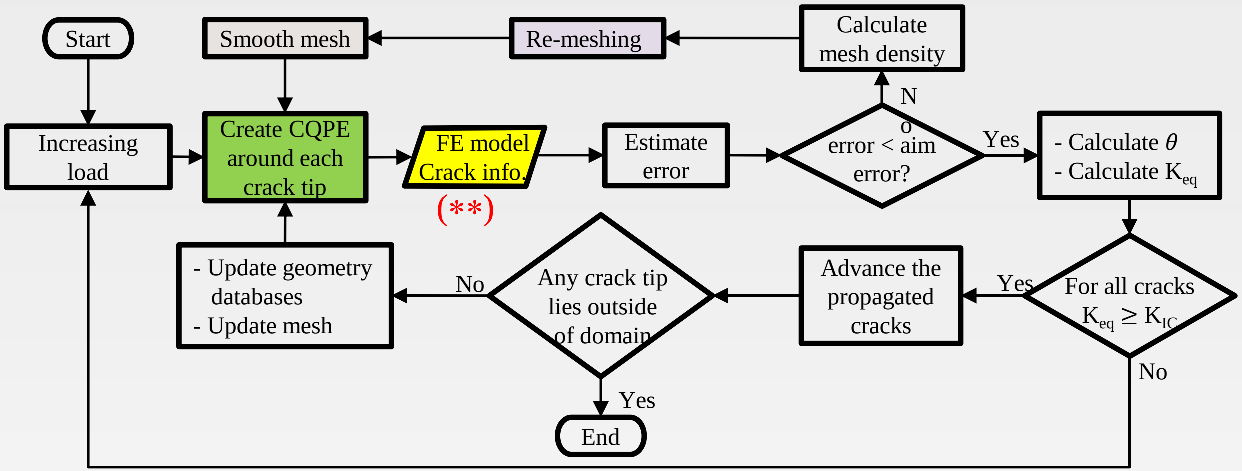

Discretization

FEM

$$\int_{\Omega}\mathbf{u}^{\mathrm{T}}\mathbf{L}^{\mathrm{T}}\mathbf{D}\mathbf{L}\mathbf{v}d\Omega+\int_{\Omega}\mathbf{b}\mathbf{v}d\Omega+\int_{\Gamma_{\mathbf{t}}}\overline{\mathbf{t}}\mathbf{v}d\Gamma=0 \quad (*)$$

Discretizing domain Ω into m finite elements that non-overlapping and conform to the crack geometry

$$\Omega\cong\Omega^{h}\equiv\bigcup_{e=1}^{m}\Omega_{e}$$

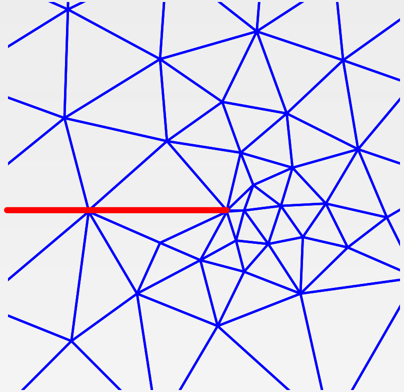

The displacement field is linearly approximated via displaced values at the three vertices

$$\mathbf{u}=\begin{Bmatrix}u\\v\end{Bmatrix}\cong\begin{Bmatrix}N_{i}u_{i}\\N_{i}v_{i}\end{Bmatrix}=\mathbf{N}\mathbf{u}_{h}^{e}$$

The discretized system

$$\mathbf{K}\mathbf{u}_{h}=\mathbf{F} \quad (**)$$

Improving the computational efficiency and accuracy of FEM → ARM

Discretization

Adaptive Remeshing

1. Posteriori error → Elements need to refine

2. Edge-split operator based on subdivision the longest edge into two new other edges

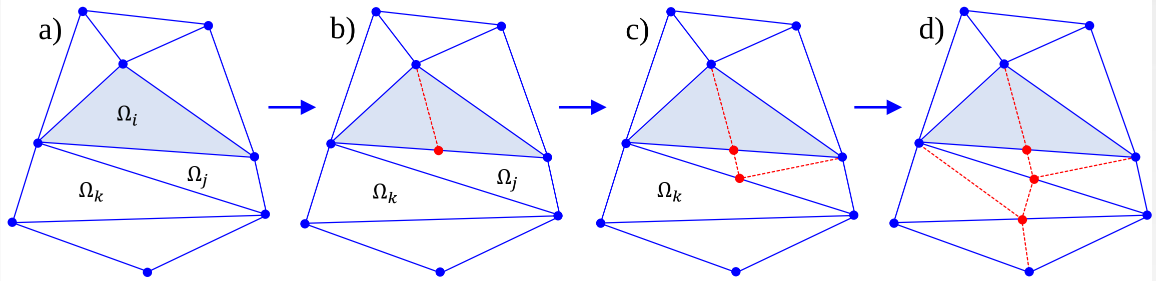

3. Remesh around each crack tip

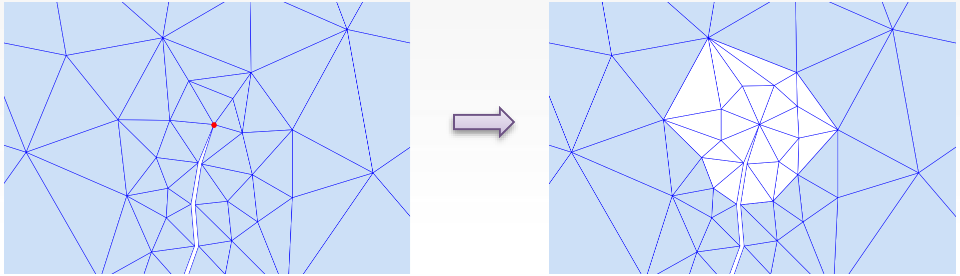

H. Dang-Trung. “Numerical investigation of fracture propagation due to slip”. Oslo. 8th January 2019

Discretization

Adaptive Remeshing

3. Remesh around each crack tip

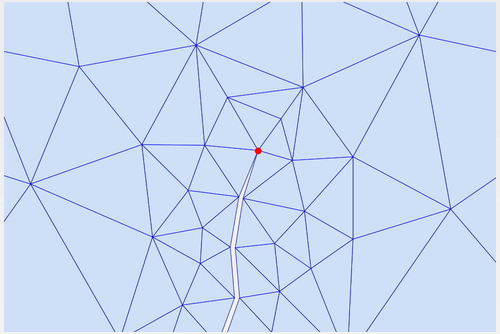

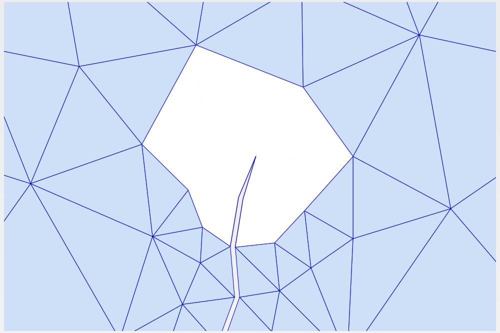

Delete domain around the tip

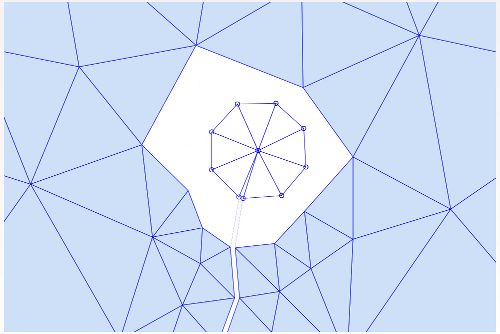

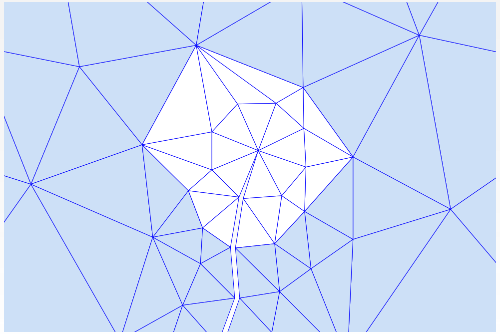

Quarter point elements around crack tip

New mesh

Playing the scales - How to upscale to a continuum scale?

- Homogenization
- Effective medium theory
- Numerical upscaling
- Data on upscaled parameters

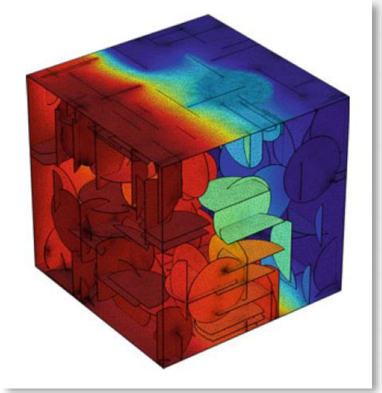

Sævik, B, Jakobsen & Lien, 2013

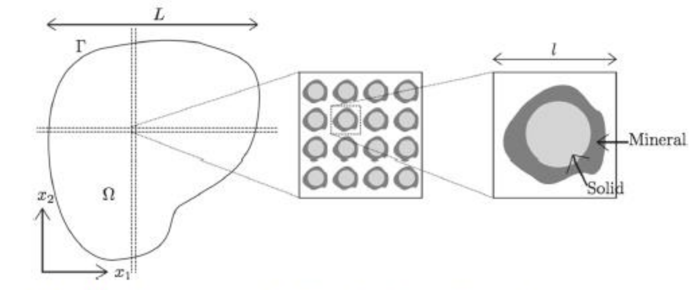

Fig. 1 Model of perforated porous medium. Typical length sizes L and l are indicated

Bringedal, B, Pop & Radu, 2016b

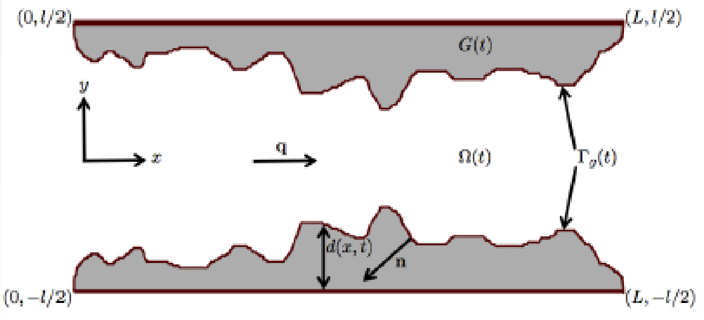

Bringedal, B, Pop & Radu, 2016a

Network based on field data

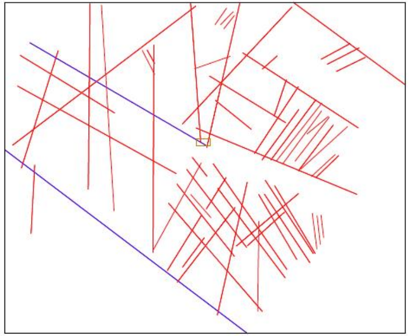

Solution along line y=0.7

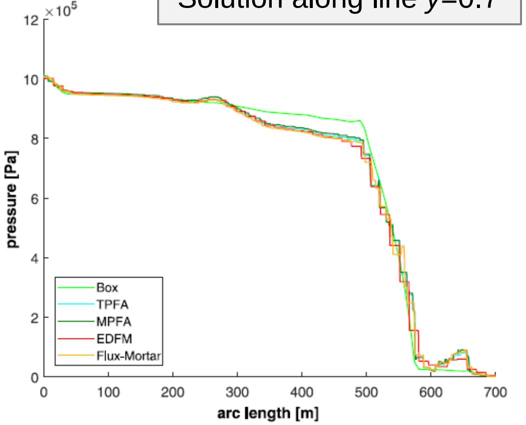

Solution along line x=625 m

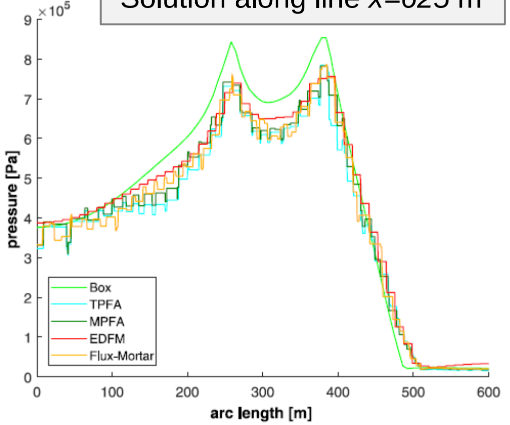

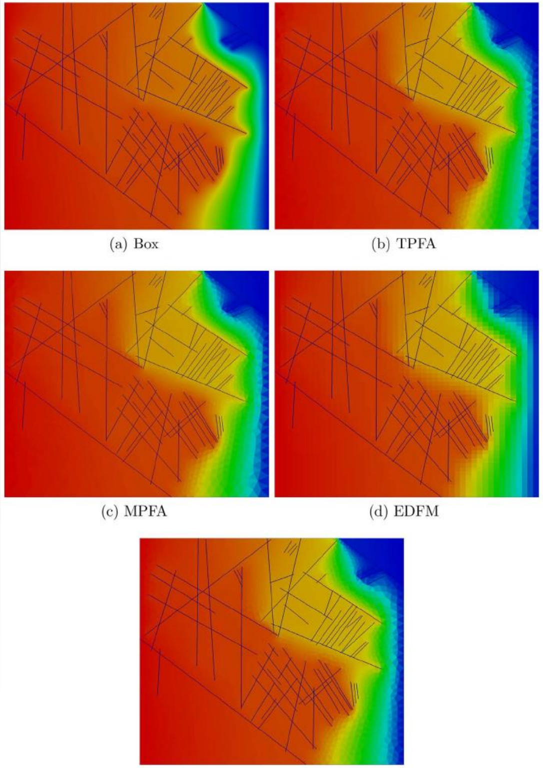

(a) Box (b) TPFA (c) MPFA (d) EDFM (e) Flux-Mortar

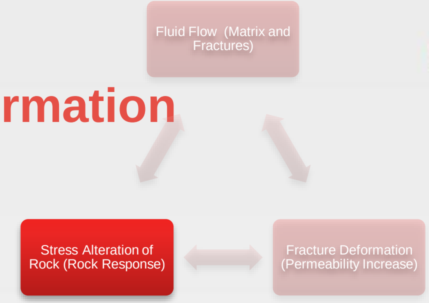

Stress response of matrix due to fracture deformation

Assumptions: quasi-static problem, isotropic medium

- Conservation of Momentum:

$$\nabla \cdot \boldsymbol{\sigma} + \mathbf{f} = 0$$

- Hooke's law

$$\boldsymbol{\sigma} = C : \boldsymbol{\varepsilon} \quad \text{where } \boldsymbol{\varepsilon} = \frac{\left(\nabla u + \left(\nabla u^{\mathrm{T}}\right)\right)}{2}$$

- Fracture deformation vector:

$$\Delta \boldsymbol{u}_f = \left(\Delta E_{n,irrev} + \Delta E_{n,rev}\right)\boldsymbol{n}_+ + \Delta d_s \boldsymbol{\tau}_+$$

- Fracture deformations conditions on internal boundaries

Numerical Approach

Cell-centered finite-volume method (MPSA) for fractured media

Ucar, Keilegavlen, Berre, Nordbotten, *Comput Geosci*, 2018

PorePy

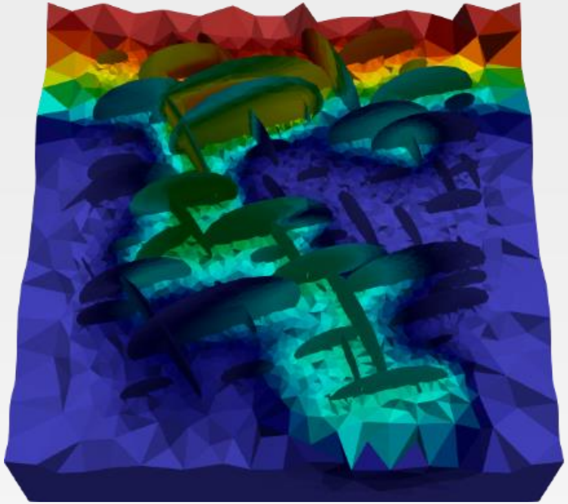

github.com/pmgbergen/porepy

Keilegavlen, Fumagalli, Berge, Stefansson, B. “PorePy: An Open-Source Simulation Tool for Flow and Transport in Deformable Fractured Rocks”, arXiv, 2017

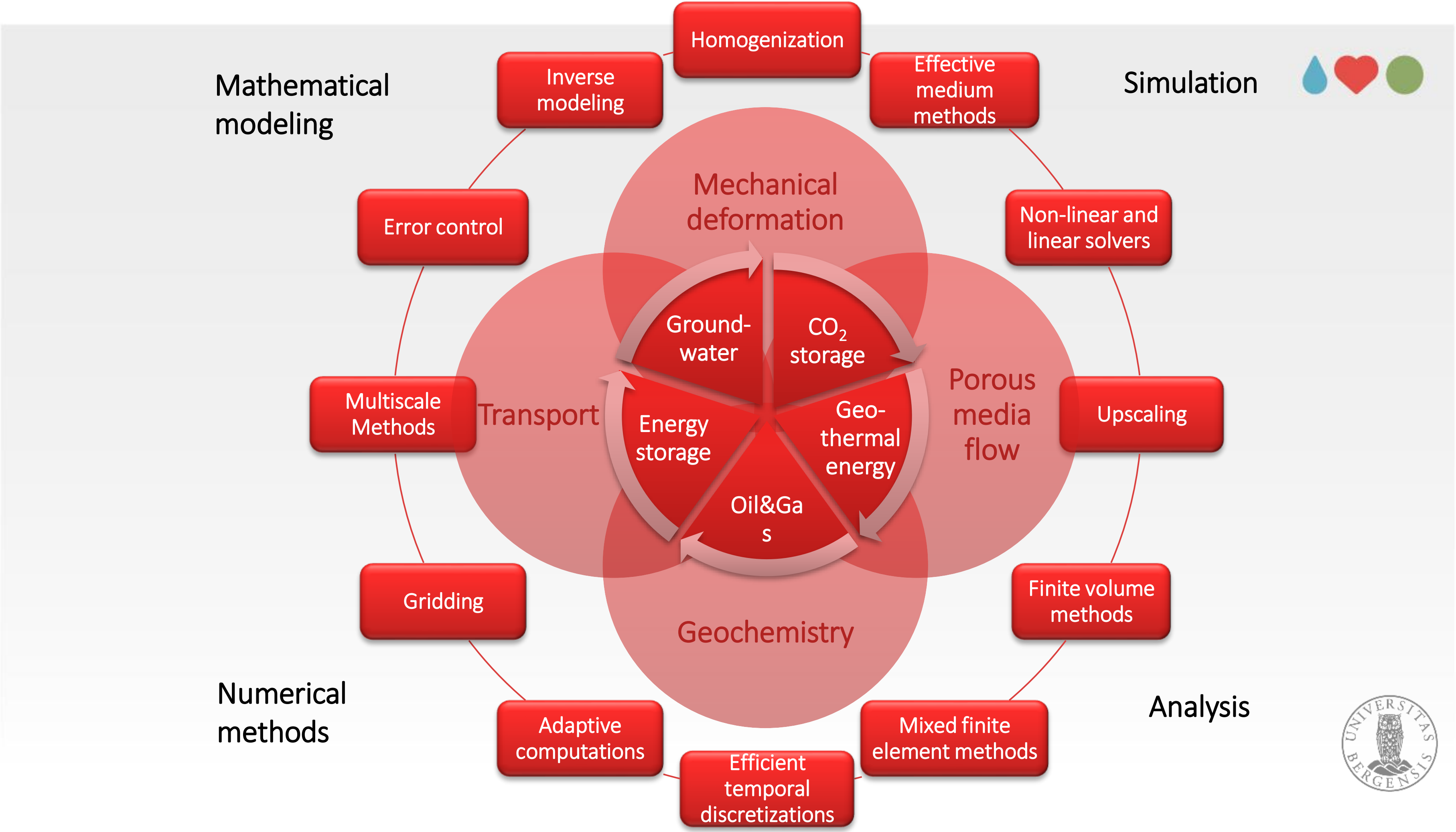
Mathematical modeling
Simulation
Numerical methods
Analysis
Homogenization
Inverse modeling
Effective medium methods
Error control
Non-linear and linear solvers
Multiscale Methods
Upscaling
Gridding
Finite volume methods
Adaptive computations
Efficient temporal discretizations
Mixed finite element methods
Mechanical deformation
Transport
Porous media flow
Geochemistry
Ground-water
CO_2 storage
Energy storage
Geo-thermal energy
Oil&Ga s